

PRESENTACIÓN MURAL

Photometric and kinematic study of the Galactic open cluster NGC 2309

A. E. Piatti^{1,4}, J. J. Clariá^{3,4} & A. V. Ahumada^{2,3,4}

(1) *Instituto de Astronomía y Física del Espacio, Buenos Aires*

(2) *Observatorio Europeo del Sur, Santiago, Chile*

(3) *Observatorio Astronómico, Universidad Nacional de Córdoba*

(4) *CONICET*

Abstract. We have obtained CCD UBVI_{KC} photometry for NGC 2309, a relatively poor open cluster (OC) projected onto a rich star field in Monoceros. Probable cluster members have been identified for the first time from sound photometric criteria. We have derived the angular radius and the fundamental cluster parameters. The resulting reddening and distance values place this object among the relatively most reddened and distant known OCs projected towards the direction of NGC 2309. A detailed version of this work can be seen in PASP, 122, 288 (2010).

Resumen. Hemos obtenido fotometría CCD UBVI_{KC} para NGC 2309, un cúmulo abierto (CA) relativamente pobre en estrellas proyectado sobre un campo estelar densamente poblado en Monoceros. Probables miembros del cúmulo han sido identificados por vez primera vez a partir de sólidos criterios fotométricos. Hemos derivado el radio angular y los parámetros fundamentales del cúmulo. Los valores resultantes del enrojecimiento y la distancia muestran que NGC 2309 es uno de los CAs conocidos relativamente más enrojecidos y distantes proyectados en la dirección de NGC 2309. Una versión detallada del trabajo puede verse en PASP, 122, 288 (2010).

1. Photometric diagrams analysis

UBVI_{KC} images of NGC 2309 were obtained with the Cerro Tololo Inter-American Observatory (Chile) 0.9 m telescope and a 2048x2048 pixel Tektronix CCD. The cluster center was statistically determined from stellar density profiles, using IRAF's tasks and applying a method developed by Piatti et al. (2005). From the resulting radial density profile an angular radius of $7.9' \pm 0.7'$ was derived. The resulting colour-magnitude diagrams (CMDs) and colour-colour diagrams (CCDs) are presented in Fig. 1(a), while Fig. 1(b) shows a close up of the ($U - B, B - V$) diagram where a sequence of stars earlier than about A0 runs nearly parallel to the unreddened CCD. By shifting the Zero-Age Main sequence (ZAMS) given by Lejeune & Schaerer (2001, LS01) according to $E(U - B)/E(B - V) = 0.72$, we find a good fit with the cluster sequence at a value of $E(B - V) = 0.32 \pm 0.02$. This value, adopted for NGC 2309, is the lowest reddening value in

the entire field. If we adopt $E(V-I)/E(B-V) = 1.25$ (Dean et al. 1978), this ratio implies $E(U-B)/E(V-I) = 0.58$. By sliding the stars according to the last reddening line in the $(U-B, V-I)$ diagram, we find a good fit for $E(V-I) = 0.42 \pm 0.03$. Furthermore, for the three CMDs we find that the Zero Age Main Sequence (ZAMS) matches the same star sequences for an apparent distance modulus of $V-M_V = 13.00 \pm 0.25$. Then, 23 probable members of NGC 2309 were identified by applying the two photometric criteria of Clariá & Lapasset (1986). Fig. 2 shows the resulting cluster fiducial main sequences (MSs) in the different CMDs and CCDs. Using the Schlegel et al. (1998) extinction maps, we conclude that the reddening across the cluster can be considered nearly uniform. Using $A_V/E(B-V) = 3.2$ and the derived cluster parameters, heliocentric and Galactocentric distances $d = 2.50 \pm 0.35$ and $R_{GC} = 10.54$ kpc were derived for NGC 2309, assuming the distance from the Sun to the center of the Galaxy to be 8.5 kpc. Finally, the solar metal content isochrone of LS01 for $\log t = 8.40 \pm 0.10$ ($t = 250$ Myr) turned out to be the one that most accurately reproduces the cluster features in the three CMDs.

It is a little surprising that a group of stars centered at $\sim (1050, 1030)$ pixels and encompassed by a circle of ~ 80 pixels in radius are field stars. Only from the stellar density point of view, one could expect that such concentration of stars were part of the cluster main body. However, we found that this is not the case. In order to look into such phenomenon in more detail, we built stellar density profiles projected onto the x and y -directions and counted stars within intervals of 100 pixels wide. We repeated this task for different I intervals from $I = 12.0$ down to 22.0 mag, in steps of $\Delta I = 1.0$ mag. Both the bottom left-hand and top right-hand panels of Fig. 3 (a) show, in dotted lines, the cumulative projected stellar density profiles. There is an important jump in the mean stellar density roughly around $x_o = 950$ pixels and $y_o = 1100$ pixels; the region delimited by $x > x_o$ and $y > y_o$ being higher in density, on average. This implies that the stellar density of the field is not uniform and also that the cluster itself seems to be located close to the transition zone between lower and higher stellar density areas. Indeed, the cluster projected stellar density profiles along the x - and y -directions (solid lines) confirm that it is centered at $\sim (970, 1300)$ pixels. In both histograms, we have added a constant in order to set the cluster's projected profiles at the minimum background level, for comparison purposes. In addition, we find similar behaviors of the star spatial distributions when considering different I magnitude intervals.

We constructed a pseudo-radial profile for the field stars centered on the cluster's center itself, with the aim to illustrate that just beside the cluster core region there exists an enhancement of field stars. We first performed star counts in boxes of 100 pixels a side distributed throughout the cluster field and we applied the method described by Piatti et al. (2006). From the resulting profile, we note that the further from the cluster center, the lower the field star density, which suggests the existence of an excess of field stars projected onto the cluster. These stars do not have magnitudes or colours compatible with those of the cluster stars. Similar results are also found by adopting, as centers for the pseudo-radial profile, other positions near the cluster core region. Therefore, NGC 2309 is another example that shows that only a star concentration in the sky does not constitute sufficient proof of the existence of an OC.

2. Analysis of proper motions

Using proper motions provided by the UCAC2 catalog (Zacharias et al. 2004), Dias et al. (2006, D06) applied a statistical method to obtain membership probabilities for 78 stars in the cluster field. Surprisingly, the stars with higher membership probabilities do not appear clumpy but sparsely distributed through the embraced field. Moreover, most of the brighter stars seem to belong to the field. The CMDs and CCDs here obtained for 48 out of the 78 stars of D06 are shown in Fig. 3 (b). We also drew the ZAMSs in solid lines once the cluster sequences were properly shifted by the cluster reddening and apparent distance modulus. The stars considered to be members by D06 ($P > 70\%$) do not seem to trace the cluster MS but rather they appear to belong to the star field. So, we believe that NGC 2309 is an example in the sense that sometimes the proper motions do not constitute by themselves proof of the existence of a star cluster.

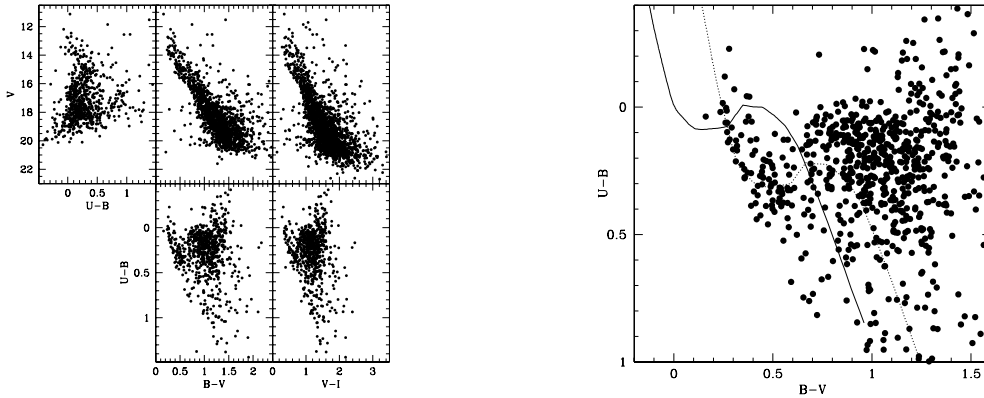


Figure 1. *Left.* CMDs and CCDs for stars in NGC 2309. *Right.* Close up of the $(U - B, B - V)$ diagram. The solid line is the unreddened ZAMS given by LS01, while the dotted line represents the reddened CC curve of the cluster.

References

- Clariá, J.J., Lapasset, E., 1986, *AJ*, 91, 326
 Dean, F.J., Warren, P.R., Cousins, A.W.J., 1978, *MNRAS*, 183, 569
 Dias, W.S., Assafin, M. et al., 2006, *A&A*, 446, 949 (D06)
 Lejeune, T., Schaerer, D., 2001, *A&A*, 366, 538 (LS01)
 Piatti, A.E., Clariá, J.J., Ahumada, A.V., 2005, *PASP*, 117, 122
 Piatti, A.E., Clariá, J.J., Ahumada, A.V., 2006, *MNRAS*, 367, 599
 Schlegel, D.J., Finkbeiner, D.P., Davis, M., 1998, *ApJ*, 500, 525
 Zacharias, N., Urban, S.E., et al., 2004, *AJ*, 127, 3043

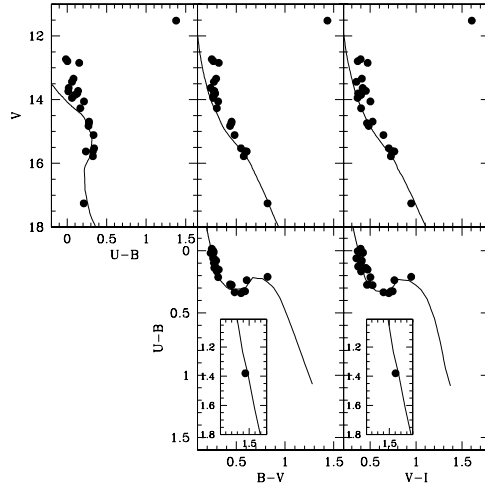


Figure 2. CMDs and CCDs for the probable members of NGC 2309. The ZAMS for luminosity class V stars is plotted as a solid line. The insets in the $(U - B, B - V)$ and $(U - B, V - I)$ diagrams show the ZAMS for luminosity class III stars overplotted.

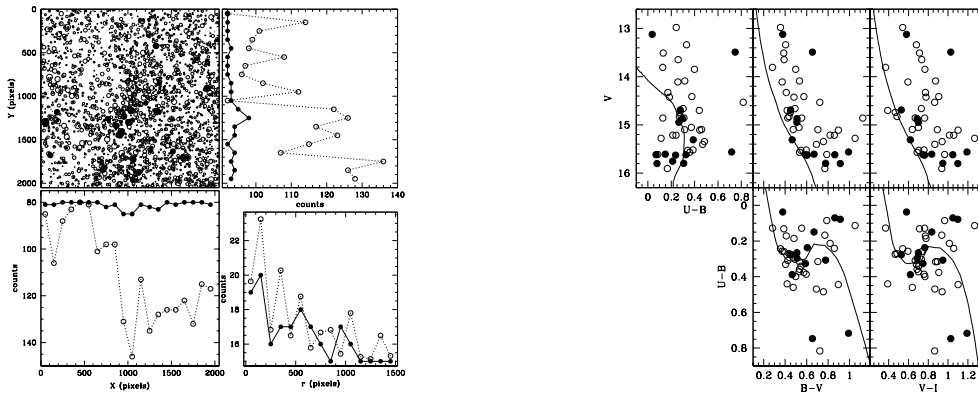


Figure 3. *Left.* a) Schematic finding chart of the stars observed in the field of NGC 2309 (top-left panel) with its projected stellar density profiles along the x (bottom-left panel) and y (top-right panel) directions, and its corresponding radial profile centered on the cluster (bottom-right panel). Open and filled circles represent field and cluster, respectively. *Right.* b) CMDs and CCDs for stars with proper motions in NGC 2309. Open and filled circles represent stars with membership probabilities lower and higher than 70%, respectively.